Journal of Controlled Release 228 (2016) 87–95

Contents lists available at ScienceDirect

Journal of Controlled Release

journal homepage: www.elsevier.com/locate/jconrel

Glucose and magnetic-responsive approach toward *in situ* nitric oxide bubbles controlled generation for hyperglycemia theranostics

Fang Yang *[,1], Mingxi Li [1], Yang Liu, Tuantuan Wang, Zhenqiang Feng, Huating Cui, Ning Gu *

State Key Laboratory of Bioelectronics, Jiangsu Key Laboratory for Biomaterials and Devices, School of Biological Sciences and Medical Engineering, Southeast University, Nanjing 210096, China

ARTICLE INFO

Article history:
Received 10 December 2015
Received in revised form 23 February 2016
Accepted 1 March 2016
Available online 4 March 2016

Keywords:
Magnetic microvesicles
Blood glucose level
Nitric oxide bubbles
Glucose oxidase
Alternating magnetic field
Diabetes

ABSTRACT

Stimuli-responsive devices that deliver drugs or imaging contrast agents in spatial-, temporal- and dosage-controlled fashions have emerged as the most promising and valuable platform for targeted and controlled drug delivery. However, implementing high performance of these functions in one single delivery carrier remains extremely challenging. Herein, we have developed a sequential strategy for developing glucose and magnetic-responsive microvesicle delivery system, which regulates the glucose levels and spatiotemporally controls the generation of nitric oxide gas free bubbles. It is observed that such injectable microvesicles loaded with enzyme and magnetic nanoparticles can firstly regulate hyperglycemic level based on the enzymatic reactions between glucose oxidase and glucose. In a sequential manner, concomitant magnetic field stimuli enhance the shell permeability while prompts the reaction between H_2O_2 and L-arginine to generate the gasotransmitters nitric oxide, which can be imaged by ultrasound and further delivered for diabetic nephropathy therapy. Therefore, magnetic microvesicles with glucose oxidase may be designed as a novel theranostic approach for restoring glucose homeostasis and spatiotemporally control NO release for maintaining good overall diabetic health.

1. Introduction

Recently, in order to establish more specific and individualized therapies for various pathologies, the promising theranostics paradigm involving a union of diagnostic and therapeutic applications into a single agent offers significant advantages over conventional drug delivery systems [1–3]. These advanced delivery systems combined diagnosis, drug delivery and treatment response are able to deliver a drug and/or contrast agent in spatial-, temporal- and dosage-controlled fashions when they are activated by specific physical (*e.g.*, external triggers like temperature [4], magnetic field [5], ultrasound [6], light [7], electric pulses [8]) or chemical (*e.g.*, endogenous changes in pH [9], enzymes [10], redox gradients [11]) triggers. Various types of carriers including organic polymers [12], inorganic/organic hybrid systems [13], and various nanoparticle [14] delivery systems have been designed to realize above mentioned unpredecendant properties. Magnetic nanoparticles (MNPs), a class of nanomaterial composed of magnetic elements, can be manipulated under the influence of an external alternating magnetic field (AMF) [15]. The magnetic properties of MNPs have been taken advantages in numerous applications related to drug and gene delivery, diagnostics and therapeutics [16–18]. Moreover, when MNPs are elaborately assembled with other multiple carriers, the magnetic composites can be developed as synergistic or sequential drug delivery systems to significantly increase delivery efficacy and reduce side effects [19,20]. However, when developing such magnetic theranostic carriers, it is still challenging to guarantee that the enhanced delivery performance at the target site (spatial control) and at the right time (temporal control) can be precisely obtained by accurate logic trigger codes.

Diabetes is a metabolic disorder that is characterized by the inability of the body to regulate blood glucose levels, among which the type 2 diabetes (non-insulin-dependent) makes up the vast majority in worldwide [21,22]. Nowadays, although a number of novel electronic devices, chemically controlled closed-loop delivery platforms, microgel, nanonetwork, *etc.* [23–25] have been developed to regulate the blood glucose effectively, it is still highly expected to identify hyperglycemia states smartly and intervene with one single dose treatment effectively. Especially, to develop an all-in-one platform combining intensive management of hyperglycemia and decreasing the incidence of complications is much more attracting. Nitric oxide (NO) is one of key biological signaling modulators in diverse physiological processes [26,27]. Deficiencies in NO production or a reduction in its bioavailability has been associated with several pathological conditions [28]. For example, some researchers have provided the evidences that NO availability in diabetes is usually decreased, and it could constitute a factor of the generalized vasculopathy present in diabetic nephropathy [29,30]. However, due to the reactive chemical nature of NO [31,32], the delivery and manipulation of NO to biological system is still a challenge. Based on

* Corresponding authors at: State Key Laboratory of Bioelectronics, Jiangsu Key Laboratory for Biomaterials and Devices, School of Biological Sciences and Medical Engineering, Southeast University, China.
E-mail addresses: yangfang2080@seu.edu.cn (F. Yang), guning@seu.edu.cn (N. Gu).
[1] These authors contributed equally to this work.

http://dx.doi.org/10.1016/j.jconrel.2016.03.002
0168-3659/

specific enzymatic reactions between glucose and glucose oxidase (GOx), we developed the glucose and magnetic-responsive nitric oxide bubble generation theranostic delivery system to regulate the glucose hemostasis as well as spatiotemporally control NO release and delivery. As shown in Fig. 1, each GOx-MMVs structure consists of L-arginine (NO pro-drug) in the inner core, magnetic nanoparticles in the shell, and GOx assembled on the surface. The GOx-MMVs carrier firstly can be used as a smart glucose stimuli system to decrease the hyperglycemia levels. Then with the help of AMF, spatiotemporally controlling the NO gas generation and delivery can be realized by invoking the reaction of H_2O_2 and L-arginine [33]. The *in situ* generated NO molecules can function as both efficient ultrasound scatters to enhance ultrasound imaging and diabetic nephropathy therapeutic agents. Thus, we expect that by both internal (glucose) and external AMF stimulating, GOx-MMVs could act as effective blood glucose level regulators and spatiotemporal reactor of NO molecules *sin vitro* and in db/db type 2 diabetes mice.

2. Materials and methods

2.1. Materials

The oleic acid-coated supermagnetic iron oxide Fe_3O_4 nanoparticles (MNPs) with a mean diameter of 12 nm were provided by the Jiangsu Key Laboratory for Biomaterials and Devices (China) [34]. Polyvinyl alcohol (PVA) (molecular weight (Mw = 31,000) was obtained from Sigma-Aldrich and poly L-lactic acid (PLLA) (Mw = 30,000) from Shandong Daigang Company (China). Sodium periodate and sodium chlorite were purchased from Shantou Xilong Chemical Company (China). L-arginine and 2′, 7′-dichlorofluorescein diacetate (DCFH-DA) were purchased from Beyotime Institute of Biotechnology (Haimen, China). 1-Ethyl-3-(3-dimethylaminopropyl) carbodiimide (EDC), N-hydroxysulfosuccinimide (NHS) sodium salt, and 2-(N-morpholino) ethanesulfonic (MES) acid were purchased from Shanghai Medpep Company (China). Glucose oxidase (GOx, G7141-10,000 U) was purchased from Sigma Aldrich (USA). Chloroform and all the other chemicals were of analytical grade and used without further purification.

2.2. Preparation and characterization of enzyme assembled magnetic microvesicles

In order to covalently couple the glucose-specific enzymes (GOx) into the magnetic microvesicles, firstly, polyvinyl alcohol (PVA) polymer (outer shell of the microvesicles) with carboxyl group was synthesized using our previous protocol [35]. Secondly, magnetic microvesicles loaded with L-arginine (MMVs) were fabricated *via* a double-emulsion method. Briefly, chloroform organic solution (10.00 mL) containing PLA (0.50 g) and oleic acid modification Fe_3O_4 superparamagnetic oxide nanoparticles (4 mg/mL, 40 μL) was emulsified with L-arginine (100 mM, 1.00 mL) solution and a little Tween 80 (about 0.05 mL) was added in the organic solution and sonicated continuously for 5 min. The first W/O emulsion is brown and visibly homogeneous. It was then poured into carboxyl group modification PVA solution (3% *w*/*v*) and mixed mechanically for 4 h to form (W/O)/W multiple emulsion MMVs. Thirdly, after separation, MMVs were suspended in MES buffer (50 mM, pH = 5.4). When activated by EDC (0.4 mg/mL) at room temperature, different concentrations of GOx (100, 200, 300, 400, 500, 600, 700, 800 μg/mL) were respectively added to and then incubated with MMVs solution at −4 °C. After 4 h, glucose oxidase modified magnetic vesicles (GOx-MMVs) were collected and washed 3 times with PBS buffer.

The mean size distribution of the GOx-MMVs was measured by particle sizing systems (AccuSizer 780 A, USA) at room temperature. The morphology and structure of the GOx-MMVs were studied by a scanning electron microscope (SEM, FEISirion-200, USA) working under acceleration voltage of 1.00 kV and a transmission electron microscope (TEM, JEOL, JEM-2000EX, Japan). Magnetization properties were studied by using a vibrating sample magnetometer (VSM, LakeShore 7407, USA) in the field H range of ±5000 Oe at room temperature.

The enzyme content adhered to magnetic vesicle was determined by the bicinchoninic acid (BCA) colorimetric protein assay. Briefly, a tertrate buffer (pH = 11.25) containing 25 mM BCA, 3.2 mM $CuSO_4$, and appropriately diluted GOx or GOx-MMVs was incubated at 60 °C for 30 min. After that the solution was cooled to room temperature, absorbance readings at 562 nm were collected by a UV–Vis 3600 spectrophotometer (Shimadzu, Japan). BSA solutions with known concentrations were used as standards. The enzymatic activity of free GOx and GOx-MMVs was tested by the Amplex® Red Glucose/Glucose Oxidase Assay Kit (Invitrogen, USA).

2.3. In vitro autonomous bubble formation

To capture the bubbles formation in real-time, GOx-MMVs samples were incubated with hyperglycemia glucose saline solution (1 mL, 400 mg/dL). The mixture was exposed to an alternating magnetic field (AMF, Shuangpin SPG-06-III) with 390 kHz frequency at room temperature, and then transferred immediately to be observed under the optical microscopy (Olympus cell TIRF, Japan) to record images over time. In order to understand the effect of AMF irradiation on the control of NO production, the various AMF exposure periods (5, 10, 15, 20, 30, 40 min) were investigated. At the same time, a fiber-optic thermometry

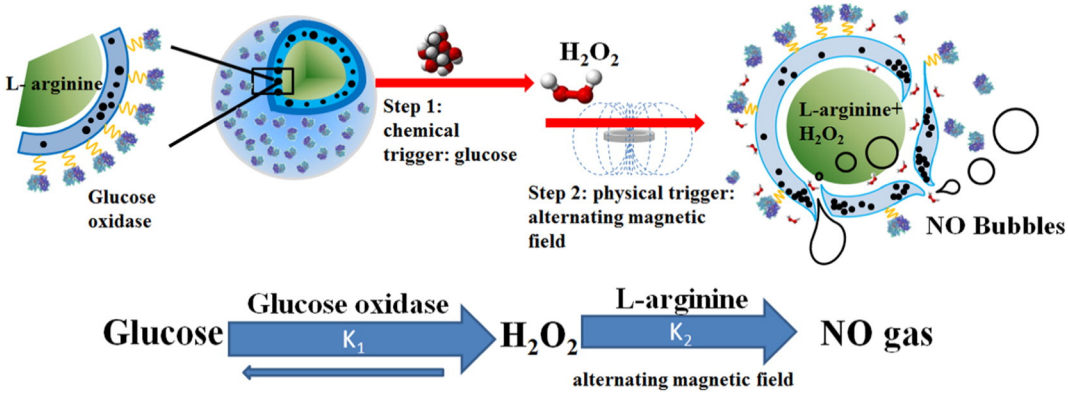

Fig. 1. Schematic diagram of microvesicles encapsulated magnetic nanoparticles and glucose oxidase for dual-stimuli responsive programmable delivery model. Firstly the encapsulated glucose-specific enzyme catalyzes glucose into gluconic acid and H_2O_2. The subsequent alternating magnetic field increases the porosity of the polymer shell, leading to the reaction between L-arginine and H_2O_2 to produce nitric oxides.

device was introduced to measure the temperature change during the AMF exposure [36].

The generated NO content was measured by using a multi-channel gas detector (IQ-1000, international sensor technology, USA). And DCFH-DA was used to dye the produced NO [37]. To assess glucose and magnetic dual-regulated release profile, GOx-MMVs reacted with glucose with and without magnetic treatment were similarly analyzed under the same conditions. Further, in order to obtain the optimal NO production, the GOx-MMVs encapsulated with different L-arginine amount (10, 100, 1000 mM) reacted with glucose solution (400 mg/dL) was studied.

The ultrasound imaging was obtained by the digital B-Mode diagnostic ultrasonic instrument Belson 3000A (Belson Imaging Technology Co., Ltd., Wu Xi, China) equipped with a 3.5 MHz R60 convex array probe. For each sample, the images of three scanned segments were processed, and then the average value of the three mean gray scales of the region of interests (ROIs) was taken as the mean gray scale of the sample. Selection and calculation of the mean gray scale for each ROI were done with Image J (NIH, USA).

2.4. In vivo glucose regulation of db/db diabetic mice

The efficacy of GOx-MMVs for glucose regulation *in vivo* was evaluated in adult type 2 db/db diabetes mice (male, from Experimental Animal Center of Yangzhou University, China). Five diabetic mice were selected for each group and administered with GOx-MMVs with and without AMF treatment, MMVs with and without AMF treatment, and control (1 × PBS) solution, respectively. All animal procedures were performed in compliance with the animal experimentation guidelines of the Animal Research Ethics Board of Southeast University.

The blood glucose levels of mice were tested continuously for two days before administration by measuring the collected tail vein blood (~3 μL) with the Accu-Chek Active Glucose Monitor (Roche, USA). GOx-MMVs solution (150 μL) was administrated by tail vein injection. The glucose level of each mouse was monitored in the first day of administration and once per day for the following days. For AMF treatment (390 kHz, 15 min), mice were exposed to the center of magnetic coil.

2.5. In vivo magnetic resonance imaging

In further, to confirm noninvasively the effective therapy of GOx-MMVs when nitric oxide was produced *in vivo*, magnetic resonance imaging (MRI) was introduced to quantify intrarenal oxygenation. The *in vivo* MRI experiments were performed using a 3.8 cm quadrature volume coil in transmit/receive mode on a 7 T small-animal MR imager (Bruker PharmaScan MRI, Germany). The mouse was positioned prone inside the coil on a heated pad with circulating water (37 °C) in the imager, with the imaging field of view (FOV) centered at the abdomen. Throughout the experiments, anesthesia was applied by inhalation of a mixture of air and 5% isoflurane.

T_2-weighted (T_2*) spin-echo images were collected with the following parameters: repetition time msec/echo time msec, 421/5; section thickness, 1 mm; 512 × 512 matrix; FOV, 3.5 × 3.5 cm^2. Synchronous with blood glucose level monitoring over time, T_2* images were monitored at the same time point. T_2* images were used as kidney anatomic reference images.

Blood oxygen level-dependent (BOLD) magnetic resonance imaging was collected by using a multi-echo T_2* gradient-echo sequence with the following parameters: 100/4–52; 10 echo times with spacing time of 5.3 ms; 30° flip angle; section thickness, 1 mm; 256 × 256 matrix; FOV, 3.5 × 3.5 cm^2. To minimize the motion artifacts from breathing, the respiratory rate of mice was maintained at about 30 breaths per minute. The decay constants of T_2* for different experimental conditions were calculated by applying an algorithm to a mono-exponential model on a pixel-by-pixel basis. ROIs that contained 15–20 pixels (about 0.25 mm^2) for cortex of both kidneys were chosen from T_2* spin-echo images. Carefully avoiding vessels and renal sinuses, three chosen ROIs were then transferred to the BOLD images to calculate a mean T_2* value in each ROI and to compare the kidney hypoxia changes before and after injection of GOx-MMVs.

2.6. Statistical analysis

The data are expressed as mean ± SD (standard deviation) unless otherwise noted. For *in vivo* studies, the data were expressed as means ± SD with a sample number of 5. Statistical analysis was performed by Student's *t*-test for two groups, and one-way analysis of variance for multiple groups. A value of $p < 0.05$ was considered as statistical significant.

3. Results and discussion

3.1. Assembly of glucose oxidase and MNPs in the microvesicles

Polymeric microvesicles with diverse structures and controlled properties have attracted much attention in targeted drug and/or contrast agent delivery due to their potential biomedical applications. Since microvesicles fabricated by polymeric assembly offers a convenient approach for cargo encapsulation, various active compounds can be sequestered into the capsule shell and/or interior [38]. Especially, incorporated or with surface-tailored inorganic nanoparticles such as gold, silica, or iron oxide in the structure make polymeric microvesicles promising as multi-stimuli responsive delivery systems [39–41]. They can be designed as programmed site-specific all-in-one approach of precise co-delivery imaging and therapeutic components. In this study, GOx-MMVs were prepared by water-in-oil-in-water (W/O/W) double emulsion-solvent evaporation method. The GOx was decorated on the shell surface of GOx-MMVs by amine and carboxyl chemical reaction [34]. Fig. S1 (Supporting Information) shows the amount of GOx adhered to MMVs plotted against the initial amount of GOx in the solution. The results demonstrated that with the increase of the amount of added GOx in the solution, the amount of GOx conjugated to MMVs increased until attained the saturation dose (510 μg/mL). Therefore, the GOx concentration of 510 μg/mL was selected as optimal enzyme loading amount on the MMVs.

The mean diameters were 2.32 ± 0.21 μm with polydispersity index of 0.09 and 2.54 ± 0.28 μm with polydispersity index of 0.11 for MMVs and GOx-MMVs, respectively (Fig. S2 shows the size distribution, Supporting Information). In order to evaluate the storage stability, the change of size and enzymatic activity of the prepared GOx-MMVs solution was observed. The results shown in Fig. S3 (Supporting Information) indicated that there was no significant size change and enzyme deactivation for the prepared GOx-MMVs solution for 7 days at −4 °C.

The surface morphology of representative SEM and TEM images was shown in Fig. 2. SEM images indicate that the MMVs without GOx modification exhibited a smooth and spherical morphology (Fig. 2a), while it was rough for the GOx modified MMVs (Fig. 2c). Compared with Fig. 2 (b, b-1), TEM images of GOx-MMVs further demonstrated that GOx was successfully decorated on the surface of MMVs. The quantities of encapsulated MNPs in microspheres were 6.21 ± 2.13%.

3.2. Validation of glucose and magnetic responsive characteristics

The magnetic performance of the GOx-MMVs was investigated at room temperature. Fig. 3a shows the magnetic hysteresis curves of the GOx encapsulated magnetic microvesicles. No remanent magnetization was observed in the curve, indicating that the superparamagnetic behavior of GOx-MMVs was preserved. As MMVs could aggregate toward the side of the cuvette nearest to the magnet, as shown in the insert of Fig. 3a, the superparamagnetic Fe_3O_4 nanoparticles embedded in the shells of microvesicles are able to spatially and temporally control the behavior of GOx-MMVs by fine-tuning the area where and the

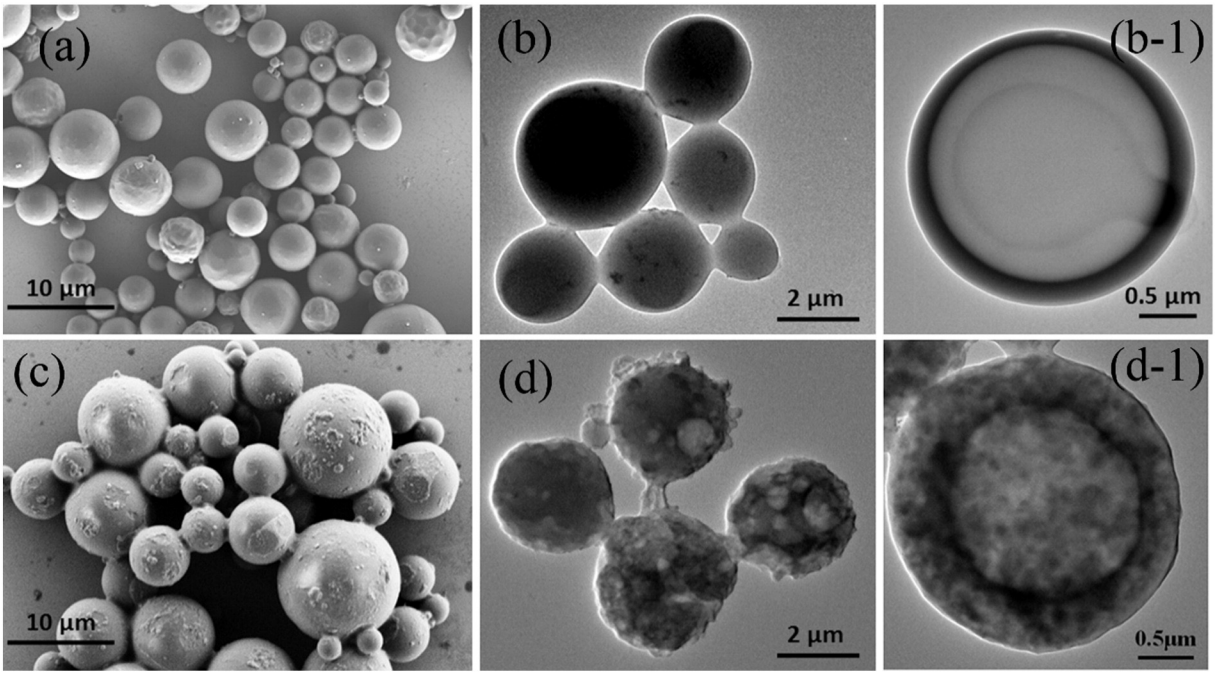

Fig. 2. SEM and TEM characterization of magnetic microvesicles. SEM images of magnetic microvesicles without (a) and with (c) glucose oxidase. TEM images of magnetic microvesicles without (b) and with (d) glucose oxidase. (b-1) and (d-1) are corresponding enlarged TEM of (b) and (d).

time when the magnetic fields are applied. As a control, no magnetic hysteresis curve was obtained for microvesicles without magnetic nanoparticle encapsulation. Prussian blue staining results in Fig. 3b showed clearly the blue colors resulting from Fe_3O_4 nanoparticles in GOx-MMVs under the optical microscopy, confirming the existence of MNPs in the microvesicles. As a result, the incorporation of MNPs into

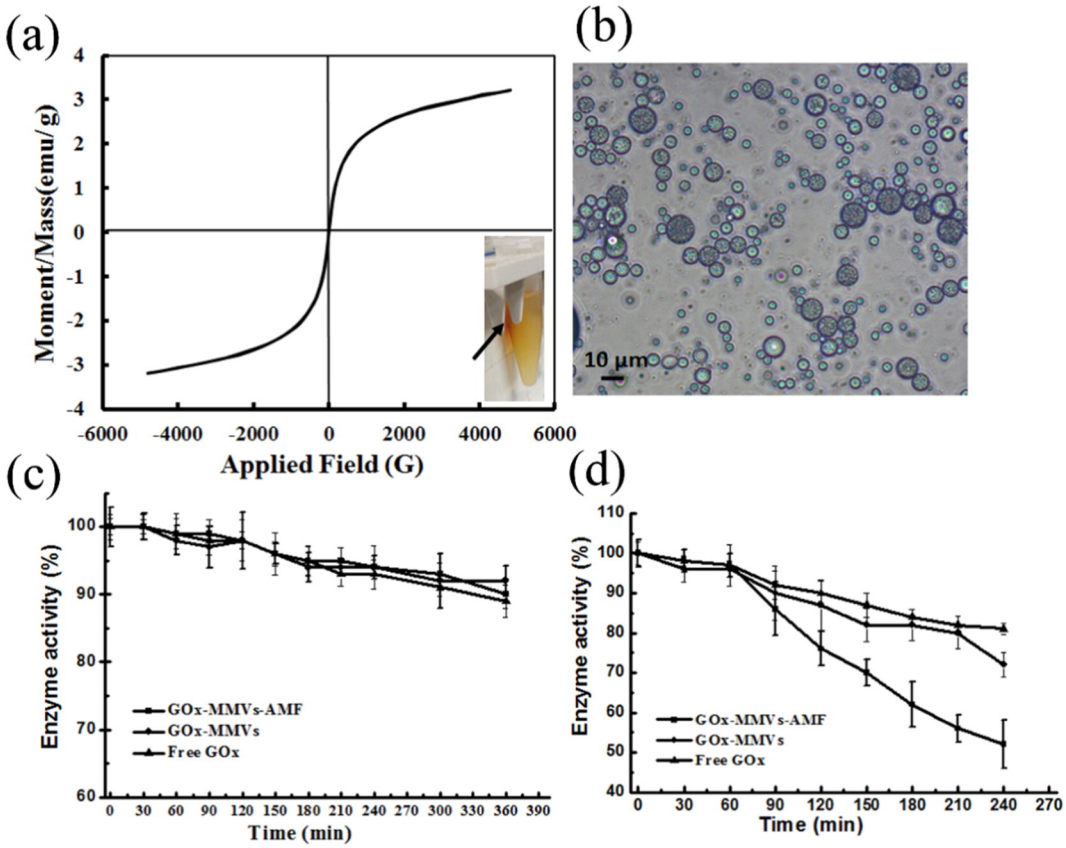

Fig. 3. Magnetic and enzymatic characterization of GOx-MMVs. (a) VSM curve of GOx-MMVs. The GOx modification on the surface of the magnetic microvesicles did not affect the superparamagnetic property. (b) Prussian blue dye microscopic image of GOx-MMVs. (c) Comparison of enzyme stabilities of free GOx, GOx-MMVs without and with AMF in PBS buffer. (d) Comparison of free GOx and GOx-MMVs incubated with a 400 mg/dL glucose saline solution with and without AMF at 37 °C for 4 h.

polymer membranes allows the controlled release of the NO production triggered by an AMF. Fig. S4 (Supporting Information) showed that when GOx-MMVs solution is exposed in AMF for 15 min, the maximum produced NO amount can be reached and at the same time, the solution temperature haven't been changed significantly. Thus, the results indicated that the optimized parameters were 510 mg/mL GOx loaded on the magnetic microvesicles and exposed to 390 kHz for 15 min. Under this condition, different concentrations of L-arginine were encapsulated into the GOx-MMVs to demonstrate the relationship between L-arginine and NO production efficiency. The results in Fig. S5 (Supporting Information) indicated that when the L-arginine concentration is 100 mM, the maximum produced NO amount can be obtained.

Moreover, in order to determine the activity of glucose oxidase after coupled on the shell of magnetic microvesicles, GOx stability and activity of GOx-MMVs samples in PBS (pH = 7.4) were tested. In a typical experiment, three samples were prepared, including the free GOx as control batch, one which was exposed to an AMF (390 KHz, 15 min) while the other one without AMF treatment. Results in Fig. 3c demonstrated that both GOx-MMVs without AMF and GOx-MMVs stimulated by AMF retained 90% of the original activity of the free GOx in PBS solution because of no reaction happened. However, when samples were put in the hyperglycemia (400 mg/dL glucose) solutions, as shown in Fig. 3d, it is interesting to see that the enzymatic reaction activity rate of GOx-MMVs samples was decreased to 50% after 4 h reaction when triggered by AMF. The reason may be that in the presence of an AMF, the vibration of the magnetic nanoparticles in the shell of microvesicles would change the shell integrity [42] and the detachment of GOx on the shell, which may influence the enzyme steric conformation leading to enzyme deactivation. These enzyme activity controlled characteristics are beneficial for maintaining the glucose hemostasis by decreasing the hyperglycemic to normoglycemic level while preventing further glucose from lowering to far below the normoglycemic level.

3.3. In vitro real time bubble capture and ultrasound imaging

To evaluate the dual stimuli effect on the GOx-MMVs, suspensions of GOx-MMVs in 400 mg/dL glucose saline solution were subjected to treatment with an AMF (390 KHz, 15 min). Fig. 4 (a, b) shows SEM images of the GOx-MMVs before and after AMF treatment. The morphology of the GOx-MMVs is clearly changed after magnetic field treatment. Fig. 4a shows that the original shell surface is relatively smooth and perfect, however, after AMF treatment, more than 90% of

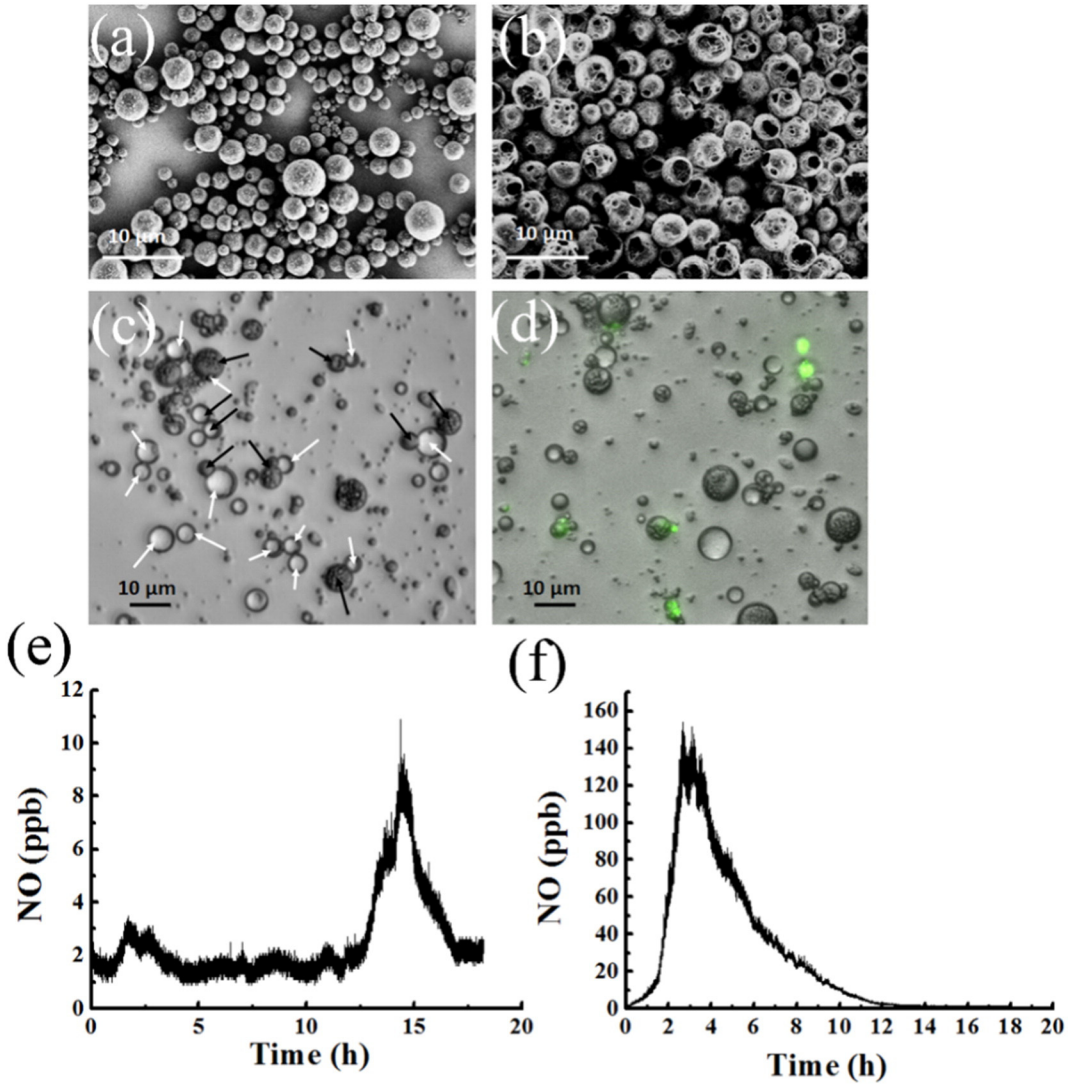

Fig. 4. Characterization of microvesicles encapsulating magnetic nanoparticles and GOx. SEM images of GOx loaded magnetic microvesicles incubation in a 400 mg/dL glucose saline solution before (a) and after (b) AMF. (c) Optical microscopic image of capturing the NO free bubbles generation (black arrows are GOx-MMVs; and white arrows are the produced microbubbles). (d) Fluorescent microscopic image of NO gas captured by DCFH-DA fluorescence. (e) and (f) are the quantitative characterization of GOx loaded magnetic microvesicles reacted in a 400 mg/dL glucose saline solution without and with AMF, respectively.

the shell surface of the GOx-MMVs are broken, as shown in Fig. 4b. An opening state of the shell may be caused by the exposure to the AMF with a concomitant nitric oxide (NO) free bubbles generation resulting from the reaction between the produced H_2O_2 and L-arginine. Optical microscopy study also confirmed the formation of spherical micrometer-sized bubbles upon exposure to hyperglycemic microenvironment and AMF activation. Fig. 4c indicated the co-existence of microvesicles and microbubbles clearly. The dynamics NO production process was also recorded by live cell optical imaging system, which demonstrated explicitly that the combined glucose and magnetic field responses took place in a sequential trigger manner to produce *in situ* microbubbles shown in Video S1 (Supporting Information).

Additionally, in order to assess NO molecules in the inner of microbubbles, DCFH-DA was used specifically to detect NO. The green fluorescence of microbubbles in Fig. 4d proved the existence of NO molecules. Fig. 4 (e, f) was the quantification of NO acquired from GOx-MMVs in a 400 mg/dL glucose saline solution without and with AMF, respectively. Without AMF treatment, the total produced NO amount was 5.64×10^{-6} μmol and to the maximum after 14.4 h reaction. Nevertheless, in the presence of AMF, the total produced NO amount was 6.33×10^{-5} μmol and to the maximum after 2.7 h reaction. The reason of delayed NO production under the without AMF irradiation condition is that glucose and AMF are sequential triggers for GOx-MMVs system. The NO generation efficacy can be controlled in a step-by-step procedure: glucose triggers first and the following AMF activation (Fig. 1). Since the NO generation is controlled in a serial manner, failure of AMF in the second step may limit the quick contact between the produced H_2O_2 and L-arginine. Thus, the NO production only can happen until L-arginine in the inner side of the microvesicles is naturally released to outside, which needs longer time under without help of AMF. However, AMF treatment makes the produced H_2O_2 quickly contact with L-arginine because of the shell permeability enhancement shown in Fig. 4b. These results quantitatively indicate the crucial role played by AMF triggering in the time and amount controlled mechanism.

As the NO molecules produced from this system increasing above the saturation concentration in the solution, the NO gas would be formed the echogenic NO free gas bubbles to enhance the ultrasound contrast imaging. A tissue-mimicking flow phantom containing a wall-less vessel was imaged with a clinical ultrasound scanner to evaluate the ultrasound imaging enhancement efficiency (Fig. 5a). The tested samples included glucose (400 mg/dL) saline solution as control, GOx-MMVs samples in glucose (400 mg/dL) saline solution with and without treatment of AMF. The ultrasonic backscatter B-mode images over time were shown in Fig. 5c. To measure the change in brightness of the ultrasound images quantitatively, a mean gray scale of all pixels within a ROI was calculated. Results shown in Fig. 5b indicated that in the presence of AMF, the ultrasound images in the whole became brighter than images in the absence of AMF. After 3 h, the ultrasound contrast enhancement efficiency reached the maximum, which is agreed with NO quantitative production result in Fig. 4f. After that, with the decrease of reaction rate, NO molecules were released from bubbles and then diffused in the solution to be undetectable by ultrasound. These results convincingly demonstrated that under the hyperglycemic glucose levels, GOx-MMVs could serve as a blood glucose regulation sensor and NO gas free bubbles production reservoir, the gate of which could be remotely controlled by logic code of glucose and AMF dual triggers. This design is engineered by two-step chemical and physical stimuli. As depicted in Fig. 1, the incorporation of glucose oxidase on the magnetic microvesicles surface has been used to gate the dosage profiles. Results in Fig. 4f demonstrated that upon hyperglycemic activation, glucose can react abruptly with glucose oxidase to produce H_2O_2 and gluconic acid in the microvesicle surface. Then AMF can be used to trigger the reaction between H_2O_2 and L-arginine *in situ* the targeted area with spatiotemporal profiles.

The magnetic field plays three roles here: (1) Since the superparamagnetic GOx-MMVs can be directed to the magnetic field in the presence of AMF, AMF can be used to realize the spatial control of GOx-MMVs to the target site; (2) AMF can help to open the shell gate quickly to stimulate the reaction between the produced H_2O_2 and

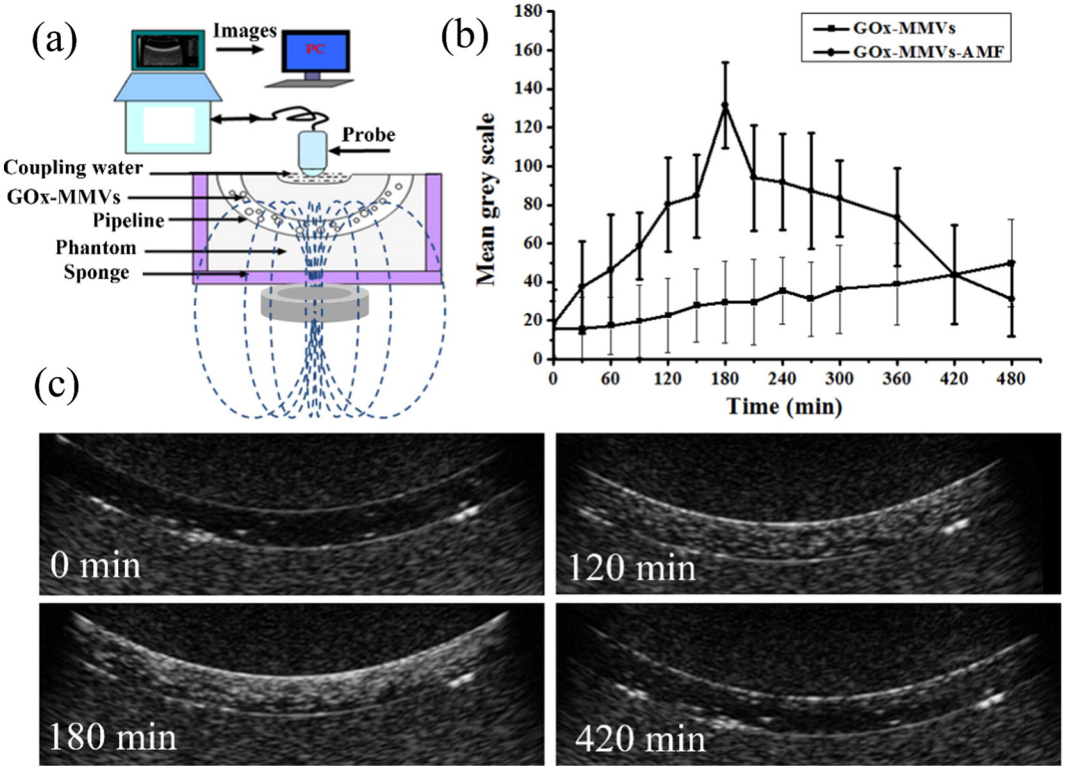

Fig. 5. *In vitro* NO free gas bubble formation of GOx-MMVs triggered by AMF and hyperglycemia status. (a) Schematic of *in vitro* ultrasound imaging experimental apparatus. (b) The quantitative mean gray scale of *in vitro* ultrasound imaging enhancement over time. (c) *In vitro* ultrasound imaging of the GOx-MMVs over time.

encapsulated L-arginine to generate NO. Since the GOx-MMVs were located in the targeted area, it also ensures that the enough NO concentration in the local sites and the rapid formation of ultrasound detectable free gas bubbles. (3) The enhanced permeability and the following disruption of the shell during the AMF treatment would in turn influence the glucose oxidase activity (Fig. 3c) to prevent the hyperglycemia status from further lowering below the normoglycemic level, which is very important for maintaining the glucose hemostasis for diabetic therapy.

3.4. Regulation of blood glucose levels in diabetes mice

We continued to assess the *in vivo* efficacy of GOx-MMVs for regulation of hyperglycemic glucose levels in db/db adult type 2 diabetic mice triggered by AMF. The db/db diabetic mice were divided into five groups and injected with GOx-MMVs with and without AMF treatment, MMVs with and without AMF treatment, as well as control (1 × PBS) solution (each mouse for 150 μL), respectively. The blood glucose levels of administrated mice in each group were then monitored over time. Fig. 6a is the schematic diagram for the *in vivo* setup. The magnetic coil was put on purpose around the mice abdomen to control the release site. As shown in Fig. 6(b, c), there is no significant glucose level decrease for MMVs with and without AMF treatment, as well as PBS treatment. However, blood glucose levels of mice injected with GOx-MMVs quickly declined to a normoglycemic state (<200 mg/dL) within 2 h after AMF (390 kHz, 15 min) treatment. Following further AMF activating, the magnetic nanoparticles in the shell of the GOx-MMVs would move within the shell to weaken the polymer shell integrity, as proved in Fig. 4. The detachment between GOx and polymer shell created more accessible sites on GOx to accelerate enzymatic oxidation of glucose at first. Compared with GOx-MMVs in the absence of AMF, the quicker decrease of glucose level was observed in those with AMF, which maintained blood glucose hemostasis in the normoglycemic range up to 24 h (Fig. 6c) and gradually increased a little within the next 6 days (Fig. 6b). The relative long term glucose hemostasis maintenance may result from two aspects. One is the ability of glucose oxidase to spontaneously and specifically react with glucose to rapidly decrease the glucose levels. Second is the NO production can be sited conversion in a controlled manner owing to following AMF trigger. Since some researchers have demonstrated that the disturbed NO metabolism represents a concause of nephropathy in diabetes [43–45], the formation of NO may be beneficial for glucose-induced insulin secretion from pancreatic islets. Therefore, both the abrupt enzyme response to the hyperglycemia condition and AMF triggered NO production prompt the longer glucose hemostasis even with single-dose injection of GOx-MMVs. The preliminary amelioration effect for hyperglycemia associated nephropathy complications was demonstrated in the following renal oxygenation magnetic resonance imaging.

3.5. In vivo magnetic resonance imaging

In order to further prove that the sequential dual stimuli can also reduce the consequences of diabetic kidney complications in db/db mice, BOLD magnetic resonance imaging was applied for noninvasive measurement of intrarenal oxygenation [46]. Results in Fig. 7 (a-1, a-2) exhibited the kidney anatomic MR images before and after GOx-MMV injection triggered by AMF over time. T_2^* value collected from BOLD images demonstrated the quantification of intrarenal oxygenation as shown in Fig. 7b. Mean T_2^* in the renal cortex of the diabetic mice at the baseline condition was significantly low, similar with previous studies [47]. For groups MMVs with and without AMF treatment, as well as PBS treatment, it demonstrates no change of mean T2* in the renal cortex of the diabetic mice. However, after injection of GOx-MMVs and under AMF exposure, increases of 37.05% and 80.88% in T_2^* value were observed in the diabetic kidneys at first and second days respectively. The T_2^* level in cortex of diabetic mice group GOx-MMVs without AMF treatment was similar to those of control group, suggesting a similar level of renal oxygenation without AMF treatment. Although a 10.96% increase was found in the cortex of diabetic mice group without AMF treatment after injection in 2 days,

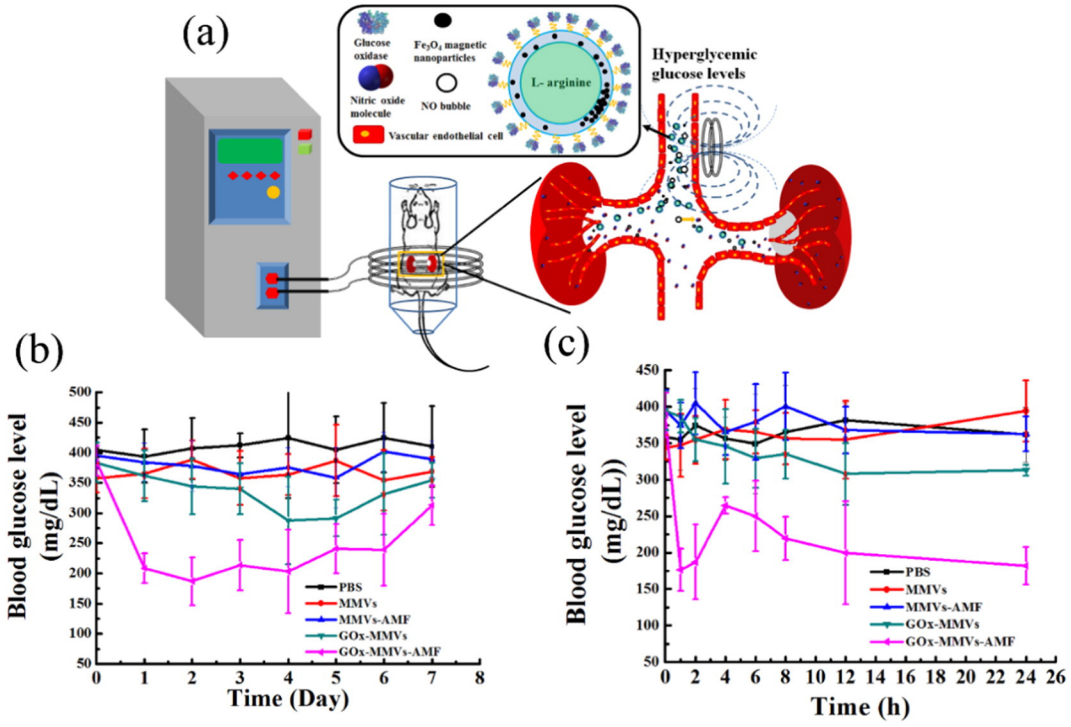

Fig. 6. AMF-mediated regulation of blood glucose levels *in vivo*. (a) Schematic of the experimental apparatus. The abdomens of anesthetized mice were immobilized in the center of magnetic coil. Blood glucose levels in db/db diabetic mice (n = 5) after tail intravenous injection with PBS, MMVs and GOx-MMVs with and without AMF from day 1 to day 7. The blood glucose levels were monitored every other day (designated the day for injection as day 0) (b) and on the first day (c).

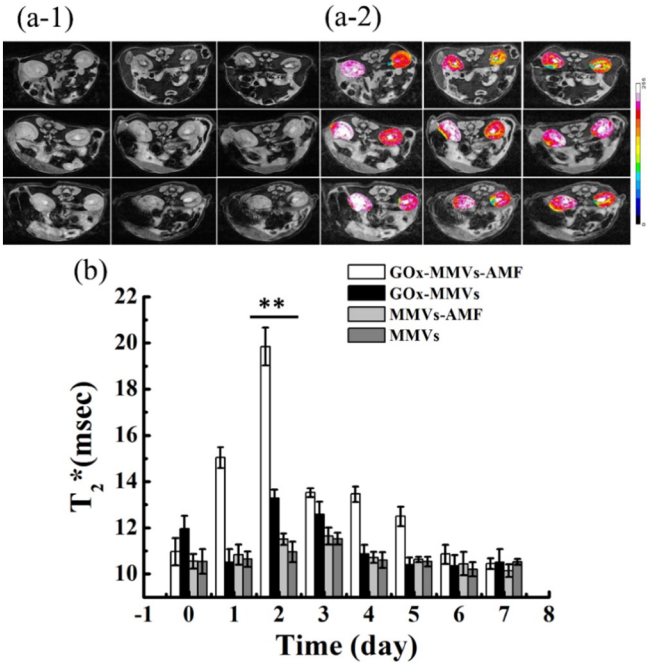

Fig. 7. *In vivo* MRI images of diabetic kidney. Before and after GOx-MMVs injection triggered by AMF over time. T_2^* images (a-1) and corresponding T_2^* intensity images (a-2). (b) Measurement of T_2^* value in the renal cortex after injection of samples.

the key differences between diabetic mice groups with and without AMF treatment are the amount and rate of NO generation shown in Fig. 4(e, f). Due to the sequential NO production based on the glucose and magnetic-responsive strategy, MRI results further demonstrated the strong inhibitory effect on high glucose-induced renal hypoxia.

Since some investigations have provided evidences that endothelial dysfunction is the key factor required for diabetic nephropathy [48], then agents that improve endothelial function or raise intraglomerular nitric oxide level could be beneficial in the treatment of diabetic nephropathy. However, the versatile chemical nature of NO and its reactivity make it difficult to be delivered directly in the body [49,50]. Thus, there is a keen interest to seek newer strategies by which NO donors can be smartly manipulated within biomaterials so that NO release and kinetic profiles can be optimized. Moreover, controlled release of short-lived NO is very important because both imaging and therapeutic effects of NO are often governed by its concentration, duration and location. In this study, upon glucose and magnetic stimuli, *in vitro* bubble capture and ultrasound imaging results shown in Fig. 4 and Fig. 5 clearly indicated the formation of NO bubbles, which demonstrates that small amount of signal gas molecules can be imaged by ultrasound based on the precise fine- tuning control. According to the chemical reaction in Fig. 1, the release kinetics of NO can be formulated in a sequential manner, which can be quantitatively described as Eqs. (1)–(2) as previously report [51].

$$[H_2O_2] = [C_{glucose}]e^{-k_1 t} \quad (1)$$

$$[NO_{gas}] = [H_2O_2]e^{-k_2 t} = [C_{glucose}]e^{-(k_1+k_2)t} \quad (2)$$

where k_1 and k_2 are the kinetic constants. According to Eq. (1), for dual stimuli strategy, the H_2O_2 can produced triggered by internal glucose levels, which can be dose controlled according to the different glucose conditions. Then following next step reaction as Eq. 2, AMF can help the immediately contact between H_2O_2 with L-arginine to spatiotemporally control nitric oxide release.

For ultrasound imaging, it may be desirable to produce NO in a higher and more sudden dose, which can be realized by sequential trigger control in this study. For therapeutics, since the NO after liberation from the microbubbles is extremely unstable and thus only locally active, the targeting control is also very important for NO therapeutics. We demonstrate herein the NO bubbles can be produced *in situ* around GOx-MMVs (Supporting Information Video S1). During this process, spatiotemporally activating the NO donor, L-arginine, needs to release NO at a sufficiently fast rate to be used as detectable ultrasound contrast agents at the targeted area by the intrinsic conversion of GOx-MMVs structure. The external magnetic field located around the abdomen can passively target NO molecules into the kidney over a therapeutically meaningful time. When the dissolved NO molecules in the blood vessel were delivered into the kidney, it is helpful for alleviating the endothelial dysfunction of diabetic renal disease proved by MR imaging of the kidney, as shown in Fig. 7. Although modulation of NO production is not yet a common therapeutic strategy, the experimental proofs have been primarily demonstrated as potential interventions to treat the nephropathy in diabetes in this study. Especially, based on one single intrinsic conversion of GOx-MMVs delivery platform activated by glucose and magnetic field, both the direct glucose decrease and indirect NO therapeutic effects benefit for long-lasting control of hyperglycemia that persist beyond the period of glycemic control.

4. Conclusions

In summary, we have developed a design based on assembling glucose oxidase and magnetic nanoparticles into a single and well-defined polymer microvesicle unit as a smart and extreme versatile all-in-one delivery platform to effectively lower glucose and prompt the therapeutic effect for hyperglycemic. By fine-tuning of magnetic field and specific enzyme reaction trigger, the glucose oxidase modified magnetic microvesicles could be converted into *in situ* nitric oxide microbubbles reservoir. The nitric oxide generation process then can be diagnosed with real-time ultrasound imaging technique. After ultrasound imaging, the dissolved nitric oxide molecules can be delivered into the targeted location to play therapeutic roles. *In vivo* results show that such sequential *in situ* conversion is possible in db/db type 2 diabetic mice for dose regulation of hyperglycemic levels and NO therapy for renal hypoxia. With this spatiotemporally control, GOx-MMVs delivery system can potentially be used as new class of promising attractive systems for the future noninvasive, rapid, and controlled regulation of glucose hemostasis. Given the fact of complex spatiotemporal control characteristics triggered by both external and internal triggers, future experiments will need to optimize the accurate balance and predictability of glucose levels in the blood and nitric oxide therapeutic functions. Furthermore, bio-safety in larger amounts of animals will also be tested.

Supplementary data to this article can be found online at http://dx.doi.org/10.1016/j.jconrel.2016.03.002.

Acknowledgements

This investigation was financially funded by the project of the National Key Basic Research Program of China (2011CB933503), the National Natural Science Foundation of China (31370019). Partial funding came from the Author of the National Excellent Doctoral Dissertation of China (201259), as well as from the Fundamental Research Fund for the Central Universities. We are grateful for the support from Collaborative Innovation Center of Suzhou Nano Science and Technology. Additionally, really appreciate Prof. Mark E. Meyerhoff of University of Michigan for the guidance of nitric oxide sensor design as well as Dr. Lina Song and Prof. Yu Zhang to provide the oleic acid Fe_3O_4 superparamagnetic iron oxide nanoparticles and valuable discussions. Thankful for Dr. Fengchao Zang and Prof. Gaojun Teng from Jiangsu Key Laboratory of Molecular and Functional Imaging for the mice magnetic resonance imaging experiment.

References

[1] T. Dreifuss, O. Betzer, M. Shilo, A. Popovtzer, M. Motiei, R. Popovtzer, A challenge for theranostics: is the optimal particle for therapy also optimal for diagnostics? Nanoscale 7 (2015) 15175–15184.
[2] S.K. Patel, J.M. Janjic, Macrophage targeted theranostics as personalized nanomedicine strategies for inflammatory diseases, Theranostics 5 (2015) 150–172.
[3] K. Park, Controlled drug delivery systems: past forward and future back, J. Control. Release 190 (2014) 3–8.
[4] B. Jeong, S.W. Kim, Y.H. Bae, Thermosensitive sol–gel reversible hydrogels, Adv. Drug Deliv. Rev. 54 (2002) 37–51.
[5] E. Bringas, O. Koysuren, D.V. Quach, M. Mahmoudi, E. Aznar, J.D. Roehling, M.D. Marcos, R. Martinez-Manez, P. Stroeve, Triggered release in lipid bilayer-capped mesoporous silica nanoparticles containing SPION using an alternating magnetic field, Chem. Commun. 48 (2012) 5647–5649.
[6] J. Di, J. Price, X. Gu, X. Jiang, Y. Jing, Z. Gu, Ultrasound-triggered regulation of blood glucose levels using injectable nano-network, Adv. Healthc. Mater. 3 (2014) 811–816.
[7] S. Shah, P.K. Sasmal, K.B. Lee, Photo-triggerable hydrogel-nanoparticle hybrid scaffolds for remotely controlled drug delivery, J. Mater. Chem. B Mater. Biol. Med. 2 (2014) 7685–7693.
[8] Y. Li, R.S. Shawgo, B. Tyler, P.T. Henderson, J.S. Vogel, A. Rosenberg, P.B. Storm, R. Langer, H. Brem, M.J. Cima, *In vivo* release from a drug delivery MEMS device, J. Control. Release 100 (2004) 211–219.
[9] J. Liu, Y. Huang, A. Kumar, A. Tan, S. Jin, A. Mozhi, X.J. Liang, pH-sensitive nano-systems for drug delivery in cancer therapy, Biotechnol. Adv. 32 (2014) 693–710.
[10] Y. Elani, R.V. Law, O. Ces, Vesicle-based artificial cells as chemical microreactors with spatially segregated reaction pathways, Nat. Commun. 5 (2014) 5305.
[11] A. Wang, M. Guo, N. Wang, J. Zhao, W. Qi, F. Muhammad, L. Chen, Y. Guo, N.T. Nguyen, G. Zhu, Redox-mediated dissolution of paramagnetic nanolids to achieve a smart theranostic system, Nanoscale 6 (2014) 5270–5278.
[12] G. Qing, M. Li, L. Deng, Z. Lv, P. Ding, T. Sun, Smart drug release systems based on stimuli-responsive polymers, Mini Rev. Med. Chem. 13 (2013) 1369–1380.
[13] Y. Li, T.Y. Lin, Y. Luo, Q. Liu, W. Xiao, W. Guo, D. Lac, H. Zhang, C. Feng, S. Wachsmann-Hogiu, J.H. Walton, S.R. Cherry, D.J. Rowland, D. Kukis, C. Pan, K.S. Lam, A smart and versatile theranostic nanomedicine platform based on nanoporphyrin, Nat. Commun. 5 (2014) 4712.
[14] S.H. Hu, S.Y. Chen, X. Gao, Multifunctional nanocapsules for simultaneous encapsulation of hydrophilic and hydrophobic compounds and on-demand release, ACS Nano 6 (2012) 2558–2565.
[15] V.I. Shubayev, T.N. Pisanic, S. Jin, Magnetic nanoparticles for theragnostics, Adv. Drug Deliv. Rev. 61 (2009) 467–477.
[16] J. Huang, M. Guo, H. Ke, C. Zong, B. Ren, G. Liu, H. Shen, Y. Ma, X. Wang, H. Zhang, Z. Deng, H. Chen, Z. Zhang, Rational design and synthesis of gamma Fe_2O_3@Au magnetic gold nanoflowers for efficient cancer theranostics, Adv. Mater. 27 (34) (2015) 5049–5056.
[17] W. Cai, X. Chen, Nanoplatforms for targeted molecular imaging in living subjects, Small 3 (2007) 1840–1854.
[18] M.K. Yu, J. Park, S. Jon, Targeting strategies for multifunctional nanoparticles in cancer imaging and therapy, Theranostics 2 (2012) 3–44.
[19] A. Curcio, R. Marotta, A. Riedinger, D. Palumberi, A. Falqui, T. Pellegrino, Magnetic pH-responsive nanogels as multifunctional delivery tools for small interfering RNA (siRNA) molecules and iron oxide nanoparticles (IONPs), Chem. Commun. 48 (2012) 2400–2402.
[20] J. Estelrich, E. Escribano, J. Queralt, M.A. Busquets, Iron oxide nanoparticles for magnetically-guided and magnetically-responsive drug delivery, Int. J. Mol. Sci. 16 (2015) 8070–8101.
[21] R.R. Holman, S.K. Paul, M.A. Bethel, D.R. Matthews, H.A. Neil, 10-year follow-up of intensive glucose control in type 2 diabetes, N. Engl. J. Med. 359 (2008) 1577–1589.
[22] D.M. Nathan, Diabetes: advances in diagnosis and treatment, JAMA 314 (2015) 1052–1062.
[23] X. Chen, W. Wu, Z. Guo, J. Xin, J. Li, Controlled insulin release from glucose-sensitive self-assembled multilayer films based on 21-arm star polymer, Biomaterials 32 (2011) 1759–1766.
[24] Z. Gu, T.T. Dang, M. Ma, B.C. Tang, H. Cheng, S. Jiang, Y. Dong, Y. Zhang, D.G. Anderson, Glucose-responsive microgels integrated with enzyme nanocapsules for closed-loop insulin delivery, ACS Nano 7 (2013) 6758–6766.
[25] W. Zhao, H. Zhang, Q. He, Y. Li, J. Gu, L. Li, H. Li, J. Shi, A glucose-responsive controlled release of insulin system based on enzyme multilayers-coated mesoporous silica particles, Chem. Commun. 47 (2011) 9459–9461.
[26] J.O. Lundberg, M.T. Gladwin, E. Weitzberg, Strategies to increase nitric oxide signalling in cardiovascular disease, Nat. Rev. Drug Discov. 14 (2015) 623–641.
[27] M. Valko, D. Leibfritz, J. Moncol, M.T. Cronin, M. Mazur, J. Telser, Free radicals and antioxidants in normal physiological functions and human disease, Int. J. Biochem. Cell Biol. 39 (2007) 44–84.
[28] J. Passauer, F. Pistrosch, E. Bussemaker, Nitric oxide in chronic renal failure, Kidney Int. 67 (2005) 1665–1667.
[29] G.A. Spinas, R. Laffranchi, I. Francoys, I. David, C. Richter, M. Reinecke, The early phase of glucose-stimulated insulin secretion requires nitric oxide, Diabetologia 41 (1998) 292–299.
[30] F. Paneni, S. Costantino, F. Cosentino, Role of oxidative stress in endothelial insulin resistance, World J. Diabetes 6 (2015) 326–332.
[31] P. Vallance, Nitric oxide: therapeutic opportunities, Fundam. Clin. Pharmacol. 17 (2003) 1–10.
[32] J. Kim, G. Saravanakumar, H.W. Choi, D. Park, W.J. Kim, A platform for nitric oxide delivery, J. Mater. Chem. B Mater. Biol. Med. 2 (2014) 341–356.
[33] F. Yang, P. Chen, W. He, N. Gu, X. Zhang, K. Fang, Y. Zhang, J. Sun, J. Tong, Bubble microreactors triggered by an alternating magnetic field as diagnostic and therapeutic delivery devices, Small 6 (2010) 1300–1305.
[34] L. Song, F. Zang, M. Song, G. Chen, Y. Zhang, N. Gu, Effective PEGylation of Fe_3O_4 nanomicelles for in vivo MR imaging, J. Nanosci. Nanotechno. 15 (2015) 4111–4118.
[35] L. Duan, F. Yang, L. Song, K. Fang, J. Tian, Y. Liang, M. Li, N. Xu, Z. Chen, Y. Zhang, N. Gu, Controlled assembly of magnetic nanoparticles on microbubbles for multimodal imaging, Soft Matter 11 (2015) 5492–5500.
[36] K. Fang, L. Song, Z. Gu, F. Yang, Y. Zhang, N. Gu, Magnetic field activated drug release system based on magnetic PLGA microspheres for chemo-thermal therapy, Colloids Surf. B Biointerfaces 136 (2015) 712–720.
[37] W.W. Cheng, Z.Q. Lin, Q. Ceng, B.F. Wei, X.J. Fan, H.S. Zhang, W. Zhang, H.L. Yang, H.L. Liu, J. Yan, L. Tian, B.C. Lin, S.M. Ding, Z.G. Xi, Single-wall carbon nanotubes induce oxidative stress in rat aortic endothelial cells, Toxicol. Mech. Methods 22 (2012) 268–276.
[38] R.A. Siegel, Stimuli sensitive polymers and self regulated drug delivery systems: a very partial review, J. Control. Release 190 (2014) 337–351.
[39] T. Pompe, S. Zschoche, N. Herold, K. Salchert, M.F. Gouzy, C. Sperling, C. Werner, Maleic anhydride copolymers-a versatile platform for molecular biosurface engineering, Biomacromolecules 4 (2003) 1072–1079.
[40] D.J. Pochan, J. Zhu, K. Zhang, K.L. Wooley, C. Miesch, T. Emrick, Multicompartment and multigeometry nanoparticle assembly, Soft Matter 7 (2011) 2500.
[41] A. Rosler, G.W. Vandermeulen, H.A. Klok, Advanced drug delivery devices *via* self-assembly of amphiphilic block copolymers, Adv. Drug Deliv. Rev. 53 (2001) 95–108.
[42] K. Fang, L. Song, Z. Gu, F. Yang, Y. Zhang, N. Gu, Magnetic field activated drug release system based on magnetic PLGA microspheres for chemo-thermal therapy, Colloids Surf. B Biointerfaces 136 (2015) 712–720.
[43] P. Tessari, Nitric oxide in the normal kidney and in patients with diabetic nephropathy, J. Nephrol. 28 (2015) 257–268.
[44] J. Leiper, M. Nandi, The therapeutic potential of targeting endogenous inhibitors of nitric oxide synthesis, Nat. Rev. Drug Discov. 10 (2011) 277–291.
[45] S.R. Vincent, Nitric oxide and arginine-evoked insulin secretion, Science 258 (1992) 1376–1378.
[46] L.P. Li, J. Lu, T. Franklin, Y. Zhou, R. Solomon, P.V. Prasad, Effect of iodinated contrast medium in diabetic rat kidneys as evaluated by blood-oxygenation-level-dependent magnetic resonance imaging and urinary neutrophil gelatinase-associated lipocalin, Investig. Radiol. 50 (2015) 392–396.
[47] X.G. Peng, Y.Y. Bai, F. Fang, X.Y. Wang, H. Mao, G.J. Teng, S. Ju, Renal lipids and oxygenation in diabetic mice: noninvasive quantification with MR imaging, Radiology 269 (2013) 748–757.
[48] T. Nakagawa, K. Tanabe, B.P. Croker, R.J. Johnson, M.B. Grant, T. Kosugi, Q. Li, Endothelial dysfunction as a potential contributor in diabetic nephropathy, Nat. Rev. Nephrol. 7 (2011) 36–44.
[49] A.B. Seabra, G.Z. Justo, P.S. Haddad, State of the art, challenges and perspectives in the design of nitric oxide-releasing polymeric nanomaterials for biomedical applications, Biotechnol. Adv. 33 (2015) 1370–1379.
[50] Q. Wang, H. Li, Y. Xiao, S. Li, B. Li, X. Zhao, L. Ye, B. Guo, X. Chen, Y. Ding, C. Bao, Locally controlled delivery of TNF alpha antibody from a novel glucose-sensitive scaffold enhances alveolar bone healing in diabetic conditions, J. Control. Release 206 (2015) 232–242.
[51] Y.S. Jo, A.J. van der Vlies, J. Gantz, T.N. Thacher, S. Antonijevic, S. Cavadini, D. Demurtas, N. Stergiopulos, J.A. Hubbell, Micelles for delivery of nitric oxide, J. Am. Chem. Soc. 131 (2009) 14413–14418.